ARTICLE NO. 80-4098

A80-076

40011
40013
40006

Coupled-Interaction Launch Behavior of a Flexible Rocket and Flexible Launcher

George E. Weeks* and Thomas L. Cost†
The University of Alabama—Tuscaloosa, University, Ala.

A numerical solution is developed for analyzing the coupled dynamic interaction behavior of a thrust-loaded flexible spinning rocket propelled along a flexible launcher. The partial diferential equations of motion describing the dynamic behavior of the system are solved using a hybrid approach. The spatial behavior of the rocket is modeled by the finite-element method as a beam column with sectionally constant cross-section properties, while a summation of the natural mode solutions are used to model the spatial behavior of the launcher. The resulting time-dependent differential equations, which are coupled together by consideration of the time-dependent support forces between the rocket and the launcher, are then numerically integrated in time to obtain the system transient dynamic response. Numerical results are presented which demonstrate the validity of the method and which demonstrate the influence of rocket and launcher bending flexibility on rocket launch attitude and, hence, rocket accuracy. The bending effects are shown to significantly increase unfavorable rocket launch conditions.

Nomenclature

a_x = constant acceleration of rocket along launcher
A_m, B_m = amplitude coefficients of launcher displacements [Eq. (13)]
$\{BC\}$ = rocket load vector due to thrust misalignment
e = eccentricity of mass center of rocket element (Fig. 2)
EI = bending stiffness
$\{F\}$ = rocket load vector due to mass imbalance
$[G], [K], [M]$ = gyroscopic, stiffness, and mass matrices, respectively, of rocket element
i_p = angle between principal axis and geometric centerline of rigid rocket
I_{xm}, I_{ym}, I_{zm} = mass moments of inertia of rigid rocket relative to geometric axes
J = polar mass moment of inertia of flexible rocket
$k, \bar{k}$ = spring constants of suspension (shoes) at rocket aft and fore end, respectively
l_e = length of a finite element of rocket
m = rocket mass per unit length
M = total mass of rocket
P = component of thrust parallel to rocket x axis
P_a, P_f = time-dependent aft and fore out-of-plane suspension forces, respectively
$\{R\}$ = vector of time-dependent suspension forces [Eq. (11)]
R_a, R_f = time-dependent aft and fore in-plane suspension forces, respectively
t = time
u_1, u_2 = in-plane and out-of-plane rocket displacements, respectively
$\{U\}$ = vector of time-dependent nodal point variables for entire rocket [Eq. (8)]
w_1, w_2 = in-plane and out-of-plane launcher displacements, respectively
x_1, x_2, x = inertial coordinate system of rocket (Fig. 1)
x_a, x_f = location of aft and fore rocket suspension points, respectively (Fig. 1)
y_1, y_2, y_3 = inertial coordinate system of launcher (Fig. 1)
y_a, y_f = time-dependent location of aft and fore suspension forces, respectively, on launcher (Fig. 1)
α_2, α_z = orientation of misaligned thrust vector with respect to body-fixed axes (Fig. 3)
δ = Dirac-delta function
Δt = time increment used in marching scheme of integration
$\bar{\xi}$ = location of rocket mass center with respect to body-fixed axes (Fig. 3)
ξ, η = translational coordinates of mass center of rigid rocket
ρ = launcher mass per unit length
ϕ, θ, ψ = Euler angles for rigid rocket
ϕ_m = modal functions for launcher
ω_s = natural frequency of rigid rocket on spring supports
Ω = rocket spin rate about x axis

Subscripts

a = rocket aft suspension
f = rocket fore suspension
L = launcher
R = rocket

Superscript

i = time increment relating to numerical integration

Received Aug. 22, 1979; revision received Jan. 31, 1980.

Index categories: LV/M Simulation; LV/M Structural Design (including Loads); Structural Dynamics.

*Professor of Aerospace Engineering, Dept. of Aerospace Engineering, Mechanical Engineering, and Engineering Mechanics.

†Professor of Aerospace Engineering, Dept. of Aerospace Engineering, Mechanical Engineering and Engineering Mechanics. Member AIAA.

Introduction

A DESIGN objective of all free-flight rocket systems is to lower the dispersion characteristics of the rockets.[1] One major aspect of improving system accuracy involves reducing rocket vibratory motion at the time of launch, a condition often referred to as mallaunch. To reduce this motion, the problem of accurately defining the rocket suspension forces and associated rocket-launcher interactions during the launch phase assumes major importance. For a typical rocket with a

large slenderness ratio and high spin rate, various effects such as mass unbalance and thrust misalignment[2] can cause significant bending of the rocket during the launch phase.[3] This bending of the rocket and launcher can have a marked influence on the attitude of the rocket as it leaves the launcher, and hence on the resulting accuracy.

Analyses of various aspects of flexible rocket behavior in free flight or with time-dependent constraints have appeared frequently in the literature.[4-8] However, the more encompassing problem of determining the motion of the system while the rocket is constrained by the launcher has received much less attention. Published investigations to date indicate that this problem has been treated by modeling both the rocket and the launcher as rigid bodies connected by flexible springs.[9,10] Improvements in these analyses have been made by considering the effects of a flexible rocket on a rigid launcher.[11,12] However, there still exists only qualitative agreement between theoretical results and experimental results, and it appears that an improvement of the physical modeling of the system will be required before more accurate solutions can be obtained.

The purpose of this paper is to present an analysis which can be used to quantitatively define the coupled transient dynamic response behavior of a flexible launcher-flexible rocket system with time-dependent constraints between the rocket and the launcher. Consideration of the flexibility of both the rocket and the launcher represents an improvement in the physical modeling of the system beyond current modeling practice. In particular, the rocket is modeled as an Euler beam column with sectionally constant cross-section properties described by the finite-element method, while the launcher is modeled as a uniform Euler beam which is analyzed by using modal solution techniques. The equations of motion for the rocket and launcher are then coupled by consideration of the time-dependent interacting support forces between the two components, and an algorithm for the numerical solution of these coupled equations is presented. Thrust misalignment, mass unbalance, and gyroscopic effects of the rocket are included in the analysis.

Formulation of Equations of Motion

The rocket-launcher model used in this study is illustrated schematically in Fig. 1. The rocket is supported on the launcher by linear springs located at coordinates $x=x_a$, $x=x_f$ and, as the rocket accelerates, the time-dependent positions of these contact points on the launcher are located at coordinates $y=y_a$, $y=y_f$.

Rocket

The rocket is considered as an Euler beam-column with sectionally constant cross-section properties, equal in-plane and out-of-plane bending stiffness, constant spin rate, constant mass, and constant acceleration. In addition, mass unbalance which can vary along its length as well as a thrust misalignment at $x=0$ is included in the analysis. Torsional and axial deformations are neglected as well as the rotary inertia and transverse shear effects. With these assumptions, the equations for the in-plane and out-of-plane motion of the rocket are the same as those of an axially loaded spinning rotor with mass unbalance. These questions have been derived previously[13] and, in the interest of brevity, will not be derived here. Thus, for each differential element of the rocket (Figs. 1 and 2)

$$(EI)_R\frac{\partial^4 u_1}{\partial x^4}+P\frac{\partial^2 u_1}{\partial x^2}-2J\Omega\frac{\partial^3 u_2}{\partial x^2\partial t}+m\left[\frac{\partial^2 u_1}{\partial t^2}-e\Omega^2\cos(\Omega t+\zeta)\right]+R_a\bar{\delta}(x-x_a)+R_f\bar{\delta}(x-x_f)=0 \quad (1)$$

$$(EI)_R\frac{\partial^4 u_2}{\partial x^4}+P\frac{\partial^2 u_2}{\partial x^2}+2J\Omega\frac{\partial^3 u_1}{\partial x^2\partial t}+m\left[\frac{\partial^2 u_2}{\partial t^2}-e\Omega^2\sin(\Omega t+\zeta)\right]+P_a\bar{\delta}(x-x_a)+P_f\bar{\delta}(x-x_f)=0 \quad (2)$$

$$P=\int -a_x m\,dx \quad (3)$$

Launcher

The launcher is assumed to be a uniform Euler beam with equal in-plane and out-of-plane bending stiffness and with no axial loading so that the equations of motion are

$$(EI)_L\frac{\partial^4 w_1}{\partial y^4}+\rho\frac{\partial^2 w_1}{\partial t^2}-R_a\bar{\delta}(y-y_a)-R_f\bar{\delta}(y-y_f)=0 \quad (4)$$

$$(EI)_L\frac{\partial^4 w_2}{\partial y^4}+\rho\frac{\partial^2 w_2}{\partial t^2}-P_a\bar{\delta}(y-y_a)-P_f\bar{\delta}(y-y_f)=0 \quad (5)$$

Equations (1-5) govern the dynamic response of the coupled rocket-launcher system. The algorithm used for their solution is presented in the next two sections of this paper.

Spatial Discretization of Equations of Motion

Rocket

Partial differential equations (1) and (2) governing the response of the rocket may be reduced to a set of ordinary differential equations by the use of the finite-element method. It appears that this is the first time this technique has been applied to the transient response problem of the rocket, and is used here because of its versatility in modeling abrupt changes

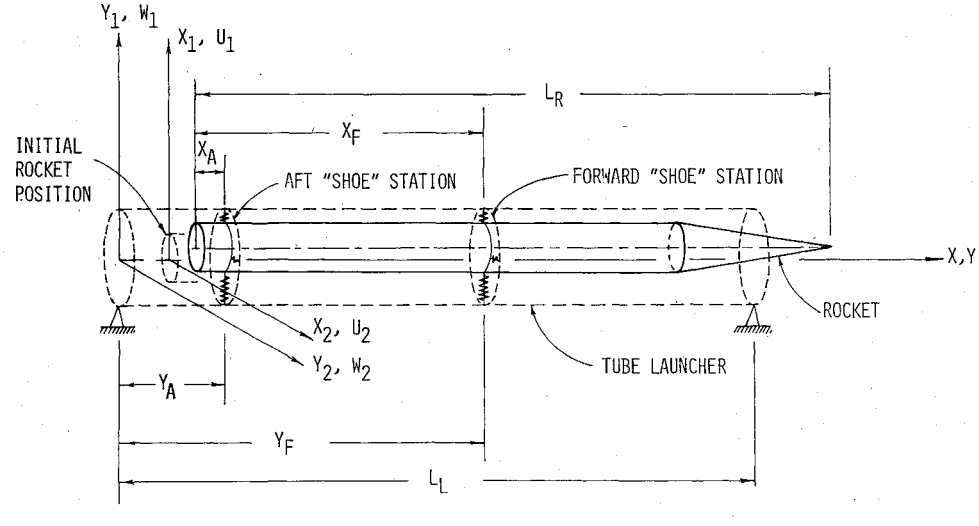

Fig. 1 Rocket and launcher inertial coordinate systems.

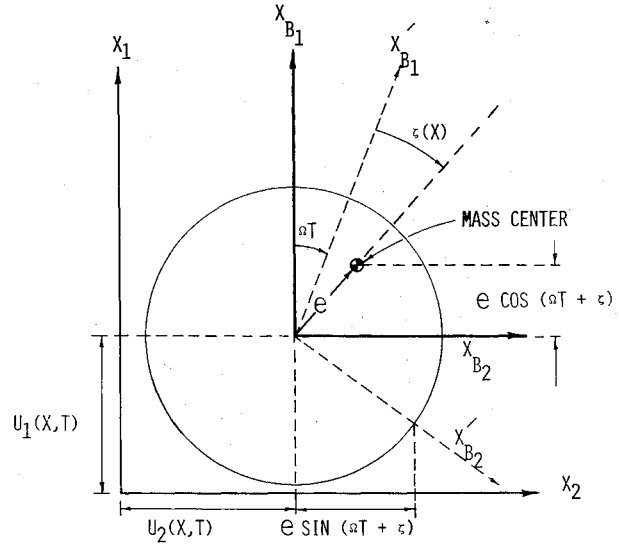

Fig. 2 Cross section of rocket with mass unbalance.

in the mass and bending stiffness that can typically occur over the length of this type of structure.

The rocket is visualized as an assemblage of Euler beam-column elements defined on subintervals $0<\xi<l_e$ and interconnected at a discrete number of nodal points along its length. For each element the appropriate equations of motion are obtained by consideration of the virtual work statement form of Eqs. (1) and (2). This virtual work statement is derived by multiplying Eqs. (1) and (2) by δu_1 and δu_2, respectively, and integrating the results by parts over the length of an element[14] to get

$$\delta W^e = 0 = \int_0^{le} \{EI(u_1''\delta u_1'' + u_2''\delta u_2'') - P(u_1'\delta u_1' + u_2'\delta u_2') + 2J\Omega(-\dot{u}_1'\delta u_2' + \dot{u}_2'\delta u_1') + m(\ddot{u}_1\delta u_1 + \ddot{u}_2\delta u_2) - me\Omega^2[\cos(\Omega t+\zeta)\delta u_1 + \sin(\Omega t+\zeta)\delta u_2]\}d\xi + \text{boundary terms} \quad (6)$$

where primes denote differentiation with respect to ξ and dots denote differentiation with respect to time. Note, importantly, the absence of the force terms R_a, R_f, P_a, P_f in Eq. (6). These terms would appear only if the support forces were present at the ends of the particular element in question.

By representing the displacements $u_1(\xi)$ and $u_2(\xi)$ as cubic polynomials in ξ, integrating over the length of each element, and summing the results,[15] the discrete equations of motion for the rocket can be written as

$$[M]\{\ddot{U}\} + [G]\{\dot{U}\} + [K]\{U\} = \{F\} + \{BC\} - \{R\} \quad (7)$$

where $\{U\}$ is

$$\{U\}^T = [\underbrace{U_1, U_1', U_2, U_2'}_{\text{Node 1}};\ \underbrace{U_1, U_1', U_2, U_2'}_{\text{Node 2}};\ldots\ldots\underbrace{U_1, U_1', U_2, U_2'}_{\text{Node } N+1}] \quad (8)$$

Symbolically, the terms in the $\{BC\}$ vector conjugate to the displacement vector $\{U\}$ [Eq. (8)] are

$$\{BC\}^T = [\underbrace{BC_1, 0, BC_2, 0}_{\text{Node 1}};\ \underbrace{0, 0, 0, 0}_{\text{Node 2}};\ \ldots\ldots;\ \underbrace{0, 0, 0, 0}_{\text{Node } N+1}] \quad (9)$$

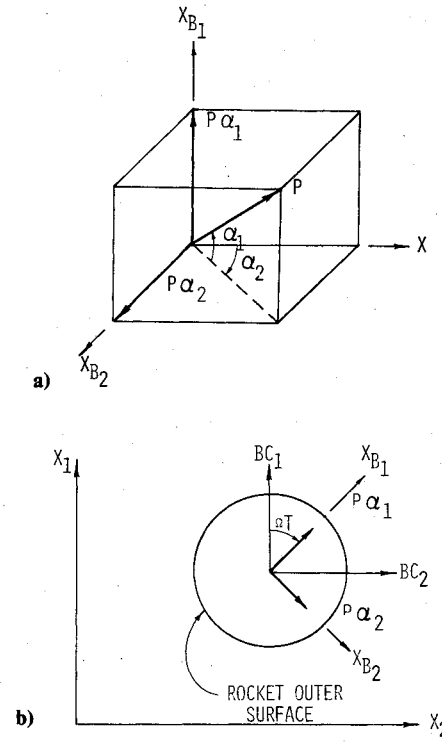

Fig. 3 Thrust components in a) body-fixed and b) inertial coordinates, assuming misalignment.

From Fig. 3, the components BC_1 and BC_2 are, for small angles of thrust misalignment,

$$BC_1 = P(\alpha_1\cos\Omega t - \alpha_2\sin\Omega t) + Pu_1'(x=0)$$

$$BC_2 = P(\alpha_1\sin\Omega t + \alpha_2\cos\Omega t) + Pu_2'(x=0) \quad (10)$$

Finally, the vector $\{R\}$ contains the time-dependent contact forces at the support points between the rocket and the launcher. Thus, for any two arbitrary but distinct nodes a and f along the rocket where the supports are located, the components of the vector $\{R\}$ conjugate to the vector $\{U\}$ [Eq. (8)] are

$$\{R\}^T = [\underbrace{0, 0, 0, 0}_{\text{Node a}};\ldots\ldots R_a, 0, P_a, 0;\ldots\ldots\underbrace{0, 0, 0, 0}_{\text{Node f}};\ldots\ldots R_f, 0, P_f, 0;\ldots\ldots 0, 0, 0, 0] \quad (11)$$

where

$$R_a = k[u_1(x=x_a) - w_1(y=y_a)]$$

$$P_a = k[u_2(x=x_a) - w_2(y=y_a)]$$

$$R_f = \bar{k}[u_1(x=x_f) - w_1(y=y_f)]$$

$$P_f = \bar{k}[u_2(x=x_f) - w_2(y=y_f)] \quad (12)$$

Launcher

Partial differential equations (4) and (5) governing the response of the launcher may be reduced to a set of ordinary differential equations by assuming a solution of the form

$$w_1(y,t) = \sum_{m=1}^{N} A_m(t)\phi_m(y) \qquad w_2(y,t) = \sum_{m=1}^{N} B_m(t)\phi_m(y) \quad (13)$$

where $\phi_m(y)$ are functions that satisfy the kinematic constraints at the ends of the launcher and at intermediate supports (if there are any) along its length. This form of solution for the spatial behavior of the launcher was used because, unlike the rocket, the mass and stiffness distribution for the launcher is relatively uniform and it was felt that sufficient accuracy could be obtained without requiring the additional degrees of freedom necessary in the finite-element method. Substituting Eq. (13) into Eqs. (4) and (5), multiplying through by $\phi_n(y)$, integrating the results over the length of the launcher, and using the orthogonality property of ϕ_m results in the equations of motion for the launcher to be

$$\ddot{A}_m + \left(\frac{EI}{\rho}\right)_L \frac{C_2}{C_1} A_m = \frac{(R_a\phi_m(y_a) + R_f\phi_m(y_f)}{C_1\rho}$$

$$\ddot{B}_m + \left(\frac{EI}{\rho}\right)_L \frac{C_2}{C_1} B_m = \frac{P_a\phi_m(y_a) + P_f\phi_m(y_f)}{C_1\rho} \qquad (14a)$$

where

$$C_1 = \int_0^L \phi_m^2(y)\,dy \qquad C_2 = \int_0^L \phi_m^{IV}(y)\phi_m(y)\,dy \qquad (14b)$$

The solution of Eqs. (7) and (14), subject to given initial conditions, defines the transient response of the rocket/launcher system. Note the equations are coupled as a result of the contact forces R_a, R_f, P_a, P_f between the rocket and the launcher.

Temporal Discretization and Solution Algorithm

Because of the complexity of Eqs. (7) and (14), an exact solution appears to be intractable and recourse to a numerical solution is necessary. For this investigation, the equations are integrated numerically in time using the constant-average-acceleration version of the Newmark temporal operator. This operator was chosen because it is unconditionally stable and allows the use of relatively large time steps in the integration procedure while still obtaining acceptable accuracy.[16] The discrete coupled equations of motion of the rocket/launcher system then become:

Rocket

$$[T]\{U\}^{(i)} = \{P\}^{(i-1)} + \Delta t^2\{\{F\}^{(i)} + \{BC\}^{(i)} - \{R\}^{(i)}\} \qquad (15)$$

Launcher

$$A_m^{(i)} = [G_m^{(i-1)} + \Delta t^2(c_m^{(i)}R_a^{(i)} + d_m^{(i)}R_f^{(i)})]/K_m$$

$$B_m^{(i)} = [H_m^{(i-1)} + \Delta t^2(c_m^{(i)}P_a^{(i)} + d_m^{(i)}P_f^{(i)})]/K_m \qquad (16)$$

where

$$[T] = 4[M] + 2\Delta t[G] + \Delta t^2[K]$$

$$\{P\}^{(i-1)} = [4[M] + 2\Delta t[G]]\{U\}^{(i-1)} + [4\Delta t[M] + \Delta t^2[G]]\{\dot{U}\}^{(i-1)} + \Delta t^2[M]\{\ddot{U}\}^{(i-1)}$$

$$G_m^{(i-1)} = 4A_m^{(i-1)} + 4\Delta t\dot{A}_m^{(i-1)} + \Delta t^2\ddot{A}_m^{(i-1)}$$

$$H_m^{(i-1)} = 4B_m^{(i-1)} + 4\Delta t\dot{B}_m^{(i-1)} + \Delta t^2\ddot{B}_m^{(i-1)}$$

$$K_m = 4 + \Delta t^2 s_m^2 \qquad s_m^2 = (EI/\rho)_L(C_2/C_1)$$

$$c_m^{(i)} = (2/L\rho)_L\phi_m(y_a) \qquad d_m^{(i)} = (2/L\rho)_L\phi_m(y_f) \qquad (17)$$

The rocket-launcher system response is now obtained by recursively solving Eqs. (15) and (16) for the rocket displacements $\{U\}^{(i)}$ and the generalized launcher displacements $A_m^{(i)}$ and $B_m^{(i)}$. Classically, this is accomplished in the following manner.[16] Assume for a moment that the force vectors $\{BC\}^{(i)}$ and $\{R\}^{(i)}$ were known as an explicit function of time. Then, by application of the initial conditions, the terms on the right-hand side of Eqs. (15) and (16) would be known so that the response at the first-time increment ($\{U\}^1$, $A_m^{(1)}$, $B_m^{(1)}$) could be calculated. Then updating the velocities and accelerations and substituting the results into the right-hand side of Eqs. (15) and (16), the response at the second-time increment ($\{U\}^{(2)}$, $A_m^{(2)}$, $B_m^{(2)}$) could be obtained. This process would be repeated as many times as necessary to trace the system response over the time interval desired.

However, it is noted that the equations of motion [Eqs. (15) and (16)] are coupled as a result of the relative displacements between the rocket and the launcher at the supports [Eq. (12)]. Since these displacements are not known a priori as an explicit function of time, it is apparent that the previously discussed procedure for recursively solving these equations must be modified to accurately reflect this coupling behavior. The appropriate modification and resulting solution algorithm used here to solve the equations of motion and, hence, to obtain the system response is developed as follows. First, the forces given by Eq. (12) are expressed in terms of the rocket displacements only. This is accomplished by substituting Eq. (16) into Eq. (13), evaluating the launcher displacements at $y=y_a$ and $y=y_f$, and solving for the contact forces in terms of these displacements. The result can be written in the form

$$R_f^{(i)} = a_1^{(i)}w_1^{(i)}(y=y_a) + a_2^{(i)}w_1^{(i)}(y=y_f) + a_3^{(i)}$$

$$R_a^{(i)} = b_1^{(i)}w_1^{(i)}(y=y_a) + b_2^{(i)}w_1^{(i)}(y=y_f) + b_3^{(i)}$$

$$P_f^{(i)} = a_1^{(i)}w_2^{(i)}(y=y_a) + a_2^{(i)}w_2^{(i)}(y=y_f) + a_4^{(i)}$$

$$P_a^{(i)} = b_1^{(i)}w_2^{(i)}(y=y_a) + b_2^{(i)}w_2^{(i)}(y=y_f) + a_5^{(i)} \qquad (18)$$

By equating the force terms in Eq. (18) to like terms in Eq. (12) the launcher displacements can be expressed in terms of the rocket displacements only. If this result is then substituted back into Eq. (12), the contact forces betweeen the rocket and the launcher can be expressed solely in terms of the rocket displacements as

$$R_a^{(i)} = E_1^{(i)}u_1^{(i)}(x=x_a) + E_2^{(i)}u_1^{(i)}(x=x_f) + E_3^{(i)}$$

$$P_a^{(i)} = E_1^{(i)}u_2^{(i)}(x=x_a) + E_2^{(i)}u_2^{(i)}(x-x_f) + E_4^{(i)}$$

$$R_f^{(i)} = E_5^{(i)}u_1^{(i)}(x=x_a) + E_6^{(i)}u_1^{(i)}(x=x_f) + E_7^{(i)}$$

$$P_f^{(i)} = E_5^{(i)}u_2^{(i)}(x=x_a) + E_6^{(i)}u_2^{(i)}(x=x_f) + E_8^{(i)} \qquad (19)$$

Next, Eq. (19) is substituted into Eq. (11) and the results into Eq. (15). The coefficients $E_1^{(i)}$, $E_2^{(i)}$, $E_5^{(i)}$, $E_6^{(i)}$ are then transposed to the left-hand side of Eq. (15) to augment the terms in the coefficient matrix $[T]$ that are conjugate to the displacements $U_1^{(i)}(x=x_a)$, $U_1^{(i)}(x=x_f)$, $U_2^{(i)}(x=x_a)$, $U_2^{(i)}(x=x_f)$. Note that the coefficients $E_1^{(i)} - E_8^{(i)}$ are defined by the development of Eqs. (18) and (19).

The solutions of Eqs. (15) and (16) are now obtained recursively as follows. By application of the initial conditions, the vectors $\{P\}^{(i-1)}$, $G_m^{(i-1)}$, $H_m^{(i-1)}$ in Eq. (17) are calculated at time $i=1$. Then with the vectors, $\{BC\}^{(i)}$ and $\{R\}^{(i)}$ given by Eqs. (9) and (11), the rocket displacements $\{U\}^{(1)}$ at the first-time increment $i=1$ are obtained by solving the system of simultaneous equations (15). These displacements are then substituted into Eq. (19) to evaluate the contact forces at time $i-1$ and the results are substituted into Eq. (16) to determine the generalized launcher displacements $A_m^{(1)}$, $B_m^{(1)}$ at the first-time increment. The velocities and accelerations are then

updated and the results are substituted into the right-hand side of Eqs. (15) and (16) to obtain the system response at the second-time increment. Continuing this procedure for as many time steps as necessary, the entire response history of the coupled transient dynamic response of the flexible rocket-flexible launcher system can be generated.

The solution procedure has been implemented in a digital computer code referred to as FLEXROK-1. The code has been written in FORTRAN-IV and computations carried out on a UNIVAC-1110 computer.

Solution Accuracy

The accuracy of the finite-element model and solution method was investigated by comparing the pitch angle and yaw rate histories of the rocket determined from the finite-element computer program FLEXROK-1 with an independently determined rigid-body dynamics solution. The assumption of rigid-body behavior corresponds to a limiting case for the finite-element method; the rocket and launcher bending stiffnesses are assumed infinitely large for this case. A validation of the finite-element solution which includes flexible bending motion was not possible since no other solutions have appeared in the literature.

Rigid-Body Solution

For purposes of validation, a rocket constructed with the goal of axial symmetry but actually possessing a slight misalignment of the principal axis (mass imbalance) was studied. For comparison with the finite-element solution, it is desirable to calculate pitch and yaw angle histories relative to an inertial frame of reference. However, the equations of motion of a rigid spinning rocket are usually expressed in terms of body-fixed coordinates such as given by Eqs. (12-34) and (12-35) of Ref. 17. Straightforward transformation of these equations to an inertial frame of reference for a rocket constrained with equal springs at its thrust end and midpoint yield

$$\ddot{\psi}+\Omega(\beta-1)\dot{\theta}=-\Omega^2\beta i_p\cos\Omega t-kL_R(\xi+L_R\psi/2)/2I_{zm}$$

$$\ddot{\theta}-\Omega(\beta-1)\dot{\psi}=\Omega^2\beta i_p\sin\Omega t+kL_R(\eta-L_R\theta/2)/2I_{zm}$$

$$\ddot{\eta}+2k\eta/M=kL_R\theta/2M$$

$$\ddot{\xi}+2k\xi/M=kL_R\psi/2M$$

$$\beta=(I_{ym}-I_{xm})/I_{zm} \qquad (20)$$

Equations (20), together with initial conditions, completely define the motion of the rigid rocket and they were solved using a fourth-order Runge-Kutta numerical solution procedure. All initial displacements and velocities were assumed zero with the exception of the rocket spin velocity.

System Parameters

The rigid-body solution and finite-element solution were evaluated for the particular case of system parameters summarized in Table 1. Dynamic unbalance is due to the principal spin axis being aligned at an angle of 10 mrad with respect to the geometric axis. The rocket is supported by shoes at its thrust end and midpoint in a nontipoff launcher.

Finite-Element Solution

A ten-element finite-element model was used to obtain the solution to the rigid-body problem. The bending stiffnesses for both the rocket and the launcher were assumed to be on the order of 10^{21} lb-in.^{2} Dynamic unbalance was prescribed by aligning the mass centers of each finite element along a line corresponding to the principal longitudinal axis of inertia. All parameters matched the rigid body system parameters described in Table 1. The pitch and yaw angles for the finite-element solution were determined by calculating the angle which a chord from the nose to the tail of the rocket makes with respect to space-fixed horizontal and vertical planes, respectively. Similarly, the pitch and yaw rates were calculated by using the linear velocities of the nose and tail nodes to calculate the rotational rates of a nose-to-tail chord.

Table 1 Validation problem system parameters

L_R = rocket length	100 in. (2.54 m)
L_L = launcher length	100 in. (2.54 m)
M = total mass	6.21 slugs (90.72 kg)
$I_{ym}=I_{zm}$ = transverse mass moments of inertia	4.31×10^3 lb-s^2-in. (48.77 kg-m^2)
I_{xm} = longitudinal mass moment of inertia	4.31×10^{-1} lb-s^2-in. (48.77×10^{-4} kg-m^2)
Ω = spin velocity	20 Hz
P = thrust (constant)	6000 lb (26.688 kN)
k = "shoe" stiffness	613,019 lb/in. (107.35 MN/m)
i_p = angle of dynamic unbalance	10 mrad

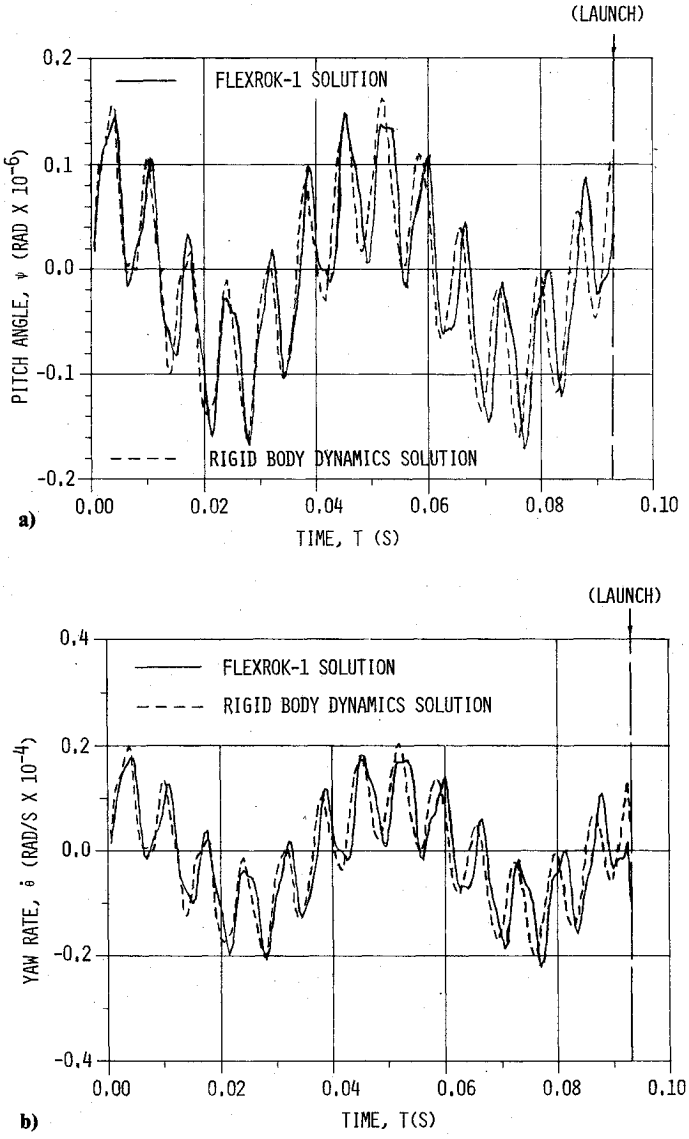

Fig. 4 Finite-element and rigid-body dynamics for a) pitch and b) yaw rate response.

Comparison of Results

Both the finite-element and rigid-body solutions were evaluated using a time step of 0.5 ms. Comparisons of the two

solutions are presented in Fig. 4 for the pitch angle and yaw rate histories. Agreement between the two solutions is remarkably good. Consideration of Fig. 4 reveals that the response history for this rigid-body case consists of a single high-frequency component superimposed on a lower frequency motion. The higher frequency motion is due to the rocket vibrating on the front and rear "shoes," while the lower frequency motion is due to the rocket spinning. The period of this motion is $1/\Omega\pi = 50$ ms, which agrees with the corresponding period determined from Fig. 4. Launch is assumed to occur at a time of 0.0929 s when the forward shoe arrives at the end of the launcher as indicated in Fig. 4.

In view of the close agreement between the finite-element solution and the independently determined rigid-body solution, it can be concluded that the transient dynamic characteristics of the finite-element solution are modeled correctly. The bending accuracy of the code was checked by applying quasistatic loads and comparing with closed-form exact solutions. Agreement in all cases was good.

Flexibility Effects on Launch Conditions

The value of the computer code FLEXROK-1 lies in its ability to calculate the influence of rocket and launcher flexibilities on the attitude of the rocket at the time of launch. This attitude, measured by both the angular rotations and rotational velocities, defines the initial conditions for a trajectory simulation computer code which may be used to study rocket accuracy. It is important to recognize that both the angular rotations and rotational velocities should be specified as initial conditions in a trajectory simulation code. As will be shown subsequently, the transition of the rocket from the guided-launch phase to the free-flight phase is a complex dynamics problem and is influenced by the rocket, launcher, and support system design. It is not sufficient to use rotational velocities only to define conditions at the time of launch.

Pitch Histories

To emphasize this point, consider a comparison of the pitch and pitch rate histories for four different rocket/launcher systems as illustrated in Fig. 5. System one is considered to be sufficiently stiff such that both the rocket and launcher may be considered rigid; system two has a flexible rocket but rigid launcher; system three a rigid rocket but flexible launcher; and system four both a flexible rocket and flexible launcher. The mass characteristics and "shoe" stiffnesses were the same in all four cases. The basis system parameters are the same as those used for the validation problem and contained in Table 1. Note that the pitch history for system one shown in Fig. 5a is so small that it appears almost zero for the scale used, although the result is the same as the finite-element solution in Fig. 4a where a larger scale is employed.

By examining Fig. 5 it is clear that the inclusion of the bending characteristics of the rocket and launcher results in significantly larger pitch angle and pitch angle rates at the time of launch. These values adversely affect the accuracy of the rocket. Also, the length of the launcher is a very important design parameter to be considered when minimizing unfavorable launch conditions. The time of launch shown in Fig. 5 depends directly on the launcher length. By choosing the launcher length such that the launch condition effects are minimized, greater accuracy could be achieved.

Parameter Study

To quantify the effects of various rocket/launcher system component flexibilities, a parameter study was conducted using the computer code FLEXROK-1. The basic system configuration studied is the nontipoff rocket/launcher configuration described in Table 1 but with varying component flexibilities. System component flexibilities were varied from by changing moments of inertia, and hence the fundamental frequencies of the various components, in an

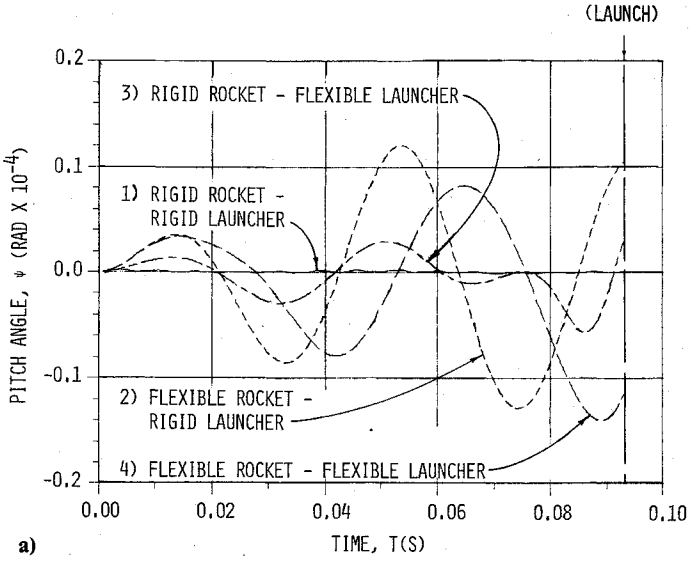

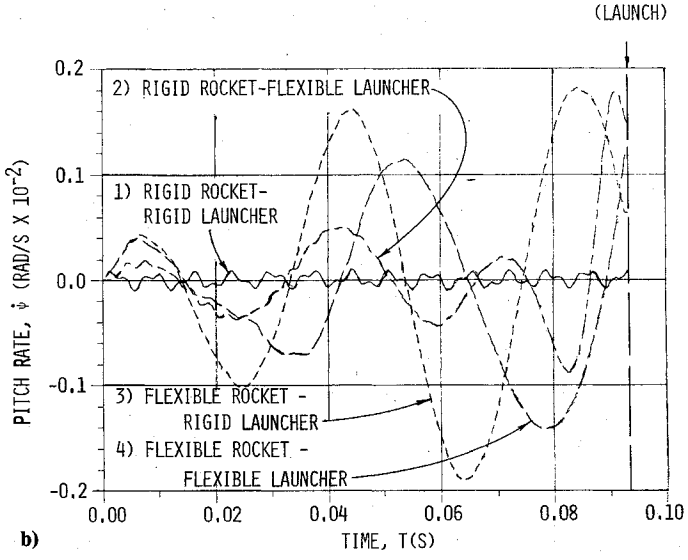

Fig. 5 Influence of rocket and launcher bending flexibilities on a) pitch and b) pitch rate.

incremental fashion. Specifically, results were obtained for rocket/launcher configurations with various combinations of the following fundamental frequencies, assuming the rocket and launcher to be simply supported beams:

$\omega_R, \omega_L =$	Case 1	Case 2	Case 3
	4.443 Hz	22.212 Hz	44.423 Hz

While it is recognized that the rocket does not correspond to a simple beam supported at its ends, the fundamental frequencies are parameters which provide a measure of the combined bending stiffness and mass characteristics of the structure.

The fundamental frequency associated with the rotation of the rocket about an axis transverse to the rocket axis is also a measure of the combined rocket inertia and stiffness of the "shoes." This frequency, $\omega_s = (1/2\pi)/(3k/M)^{1/2}$, was varied over a range from 100 to 300 Hz.

Consider the measure of mallaunch error to be used to describe the effects of the various system component flexibilities. By examining the typical responses illustrated in Fig. 5, it is clear that the specific launch angles and launch angle rates depend upon the specific time at which launch occurs. This launch time, in turn, depends upon the length of

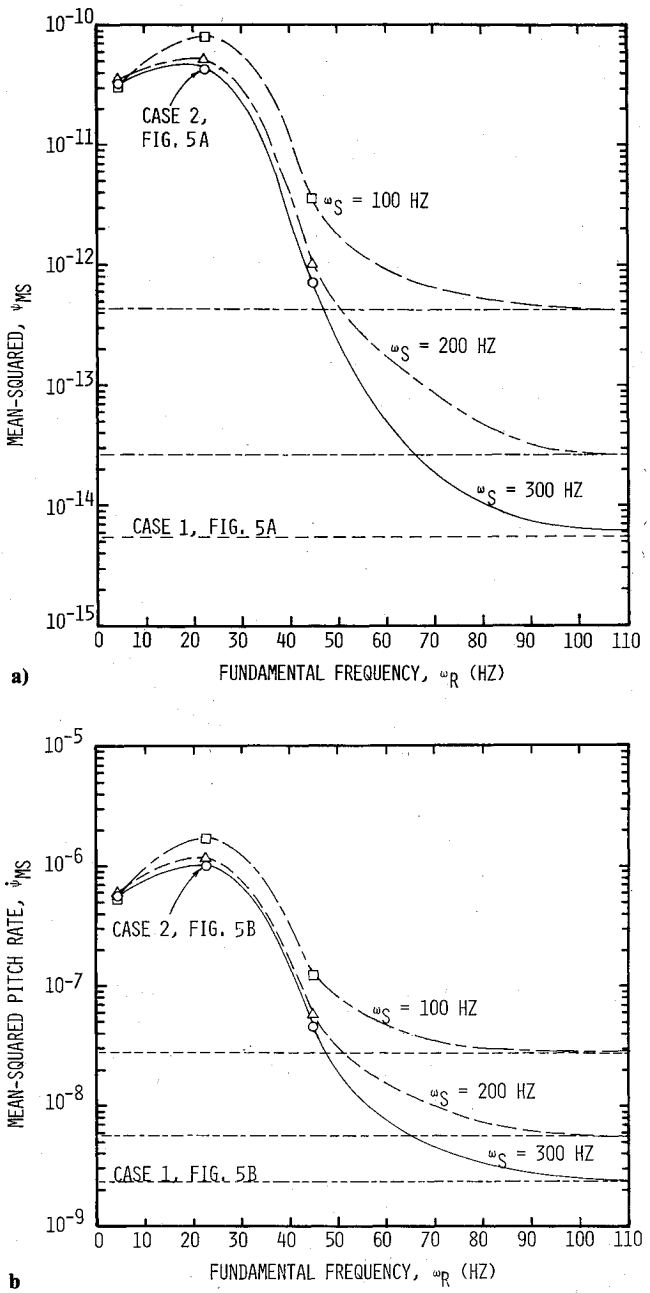

Fig. 6 Influence of rocket flexibility on a) pitch and b) pitch rate.

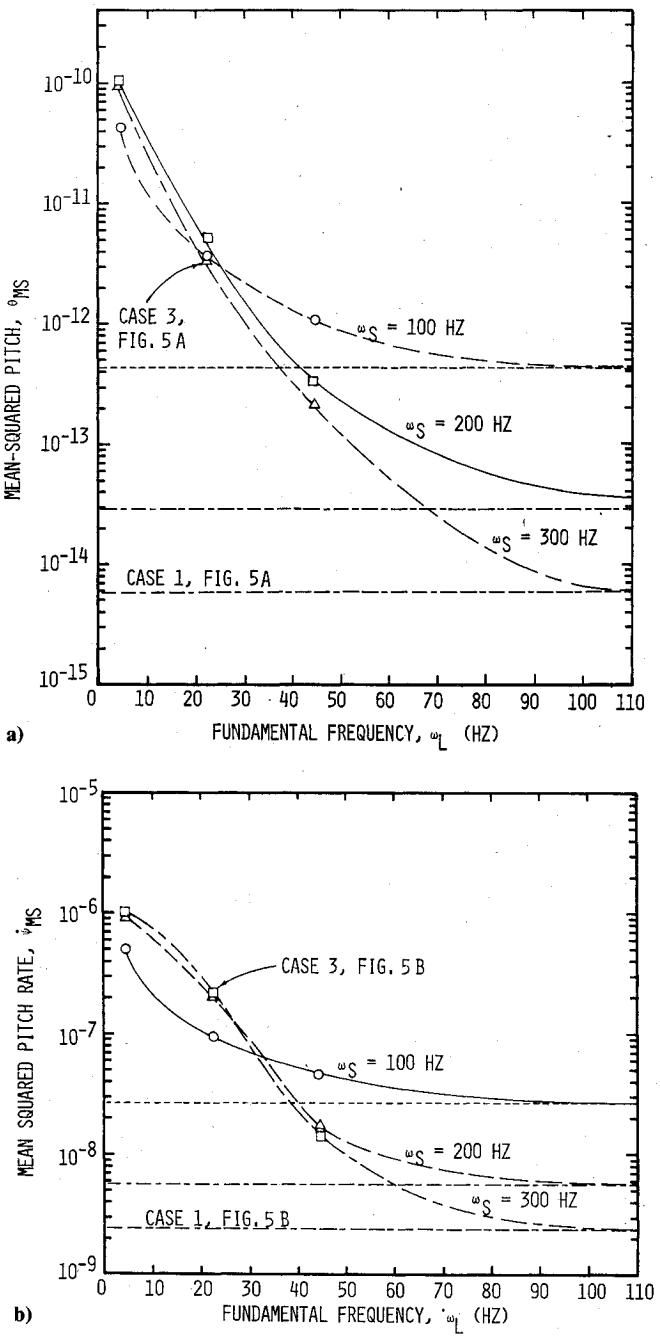

Fig. 7 Influence of launch flexibility on a) pitch and b) pitch rate.

the launcher. Since the launcher length can be easily changed, the specific values at the time of launch depend upon the specific system studied. Rather than use these specific values, the mean-squared values of the pitch and pitch rate histories were used as measures of system response. The response during the entire launch phase is summarized in terms of these mean-squared parameters. All response results are presented in terms of the mean-squared values of the pitch angles and pitch rates.

The effect of rocket flexibility, assuming the launcher is rigid, on the response variables is illustrated in Fig. 6, where both the mean-squared pitch angle and pitch angle rates are shown for various rocket fundamental frequencies. An increase in fundamental frequency corresponds to an increase in bending stiffness, assuming the mass remains constant. The three curves shown in each part of Fig. 6 represent variations in the support "shoe" stiffness. As can be seen by examining Fig. 6, as the rocket becomes more flexible the response variables become larger. The peak in the curves and subsequent decrease with decreasing frequency are due to the complicated interaction which occurs between the bending frequency behavior and rigid body oscillation. The horizontal dashed lines in Fig. 6 correspond to the case of an infinite rocket frequency.

The effect of launcher flexibility is illustrated in Fig. 7 where again it can be seen that decreasing the launcher flexibility results in a deterioration in system response. The results in Fig. 7 are based on the assumption that the rocket is rigid. The horizontal dashed lines in Fig. 7 correspond to the case of infinite launcher stiffness. The complete pitch and pitch rate histories illustrated in Fig. 5 are summarized in terms of the indicated mean-squared values in Figs. 6 and 7.

Conclusions

The finite-element analysis of a spin-stabilized flexible rocket launched from a flexible launcher presented here appears very useful. It permits the dynamic response of a complicated dynamic system involving bending of both the rocket and launcher, with associated interaction, to be

calculated in a straightforward manner. The finite-element method permits abrupt changes in the stiffness and mass characteristics along the rocket length to be modeled accurately. Furthermore, the finite-element solution has been checked by comparison with a rigid-body dynamics solution for the special case of large rocket stiffness. The favorable comparison of the finite-element results with rigid-body dynamics results for the case of appreciable rigid-body rotation represents a significant extension of the finite-element method to a new class of problems. Further applications of the finite-element method to the free-flight phase of rocket performance can be expected in the future.

The influence of both rocket and launcher bending behavior, during the launch phase of flight, on the rocket launch attitude has been demonstrated to produce a rocket with much larger pitch and yaw response during the entire launch phase of flight than if the rocket and launcher are considered rigid. This response will adversely affect rocket accuracy. Detailed design of future rocket and launcher systems should include these bending effects. Also, launcher length can be tailored to produce minimum pitch and yaw response and should be studied in system design.

Acknowledgments

The support of the U.S. Army Missile Command, Free-Flight Rocket Technology Office, Redstone Arsenal, Alabama in the conduct of this work is gratefully appreciated.

References

[1] Brown, D.B., Combs, D.R., Hahlke, C.W., and Gardner, J.P., "Free-Flight Rocket Technology Program," U.S. Army Missile Command, Redstone Arsenal, Ala., Tech. Rept. RD-76-12, July 1975.

[2] Forgey, R.W., McDermott, J.J., and Holder, D.W., "Free-Rocket Technology, Autospin, Accuracy Improvement," U.S. Army Missile Command, Redstone Arsenal, Ala., Tech. Rept. RD-75-36, June 1975.

[3] Christensen, D.E., "Multiple Rocket Launcher Characteristics and Simulation Technique," U.S. Army Missile Command, Redstone Arsenal, Ala., Tech. Rept. RL-76-11, Feb. 1976.

[4] Beal, T.R., "Dynamic Stability of a Flexible Missile Under Constant and Pulsating Thrusts," *AIAA Journal,* Vol. 3, March 1965, pp. 484-494.

[5] Meirovitch, L., "General Motion of a Variable-Mass Flexible Rocket With Internal Flow," *Journal of Spacecraft and Rockets,* Vol. 7, Feb. 1970, pp. 186-194.

[6] Meirovitch, L. and Bankovkis, J., "Dynamic Characteristics of a Two-State Variable Mass Flexible Missile With Internal Flow," NASA CR-2076, June 1972.

[7] Wilson, H.B., and Richardson, J.J., "Modal Response of Free-Rockets Under Thrust Loading," U.S. Army Missile Command, Redstone Arsenal, Ala., Tech. Rept. RL-74-2, Jan. 1974.

[8] Wu, J.J., "Missile Stability Using Finite Elements—An Unconstrained Variational Approach," *AIAA Journal,* Vol. 14, March 1976, pp. 313-319.

[9] Wempner, G.A. and Wilms, E.V., "Multirail Launcher With Six Degrees of Freedom," The University of Alabama Research Institute, Huntsville, Ala., Final Technical Report on Contract DA-01-021-AME-14042(Z), 1966.

[10] Cochran, J.E., "Investigation of Factors Which Contribute to Mallaunch of Free-Rockets," U.S. Army Research Office, Engineering Experiment Station, Auburn University, Auburn, Ala., Grant DAHCO4-75-0034, Jan. 1976.

[11] Cochran, J.E., Batson, J.L., Jr., and Christensen, D.E., "Effects of Flexibility of a Free-Flight Rocket During Launch," U.S. Army Missile Command, Redstone Arsenal, Ala., Tech. Rept. TF-77-1; *Proceedings of the Second Annual Free-Flight Rocket Workshop,* Vol. 1, Aug. 1977, pp. 27-67.

[12] Hill, J.L., Wilson, H.B., and Herron, D.J., "Optimum Attitude Control of Flexible Bodies," The University of Alabama, Tuscaloosa, Ala., Final Report, Contract DAAHO1-74-C-0833, BER Rept. 191-100, June 1975.

[13] Muszynska, A., "Nonlinear Excited and Self-Excited Precessional Vibrations of Symmetrical Rotors," in *Dynamics of Rotors,* IUTAM Symposium, edited by F.I. Niordson, Lyngby/Denmark, 1974, p. 384.

[14] Weeks, G.E. and Cost, T.L., "Dynamic Response of a Pressurized Plane Strain Cylinder Under Impulsive Distributed Loading Using Finite Element Methods," *Mechanics Research Communications,* Vol. 5, No. 2, Pergamon Press, New York, April 1978, pp. 65-71.

[15] Przemieniecki, J.S., *Theory of Matrix Structural Analysis,* McGraw-Hill Book Co., New York, 1968, p. 162.

[16] Weeks, G.E., "Temporal Operators for Nonlinear Structural Dynamics Problems," *Journal of the Engineering Mechanics Division,* ASCE, EMS, Oct. 1972, pp. 1087-1104.

[17] Kolk, W. R., *Modern Flight Dynamics,* Prentice-Hall, Inc., Englewood Cliffs, N.J., 1961, p. 231.